THE JOURNAL OF PHYSICAL CHEMISTRY B

Article

pubs.acs.org/JPCB

Raman Changes Induced by Electrochemical Oxidation of Poly(triarylamine)s: Toward a Relationship between Molecular Structure Modifications and Charge Generation

Thiago Cervantes,[†,‡] Guy Louarn,*[,‡] Henrique de Santana,[†] Lukasz Skorka,[§] and Irena Kulszewicz-Bajer*[,§]

[†]Departamento de Química, Universidade Estadual de Londrina, 86057-970 Londrina, PR, Brazil

[‡]Insitut des Materiaux Jean Rouxel, CNRS-University of Nantes, 2 rue de la Houssinière, 44322 Nantes, France

[§]Faculty of Chemistry, Warsaw University of Technology, Noakowskiego 3, 00-664 Warsaw, Poland

Supporting Information

ABSTRACT: Linear, alternating polymers of aromatic amines (*p*-phenylenediamine, bis(*p*-aminophenyl)amine, and diaminocarbazole) and either *m*-phenylene or 3,5-pyridine have been synthesized and characterized by electrochemical and spectroscopic means. The presence of radical cations in their electrochemically oxidized forms is manifested by new bands in the UV−vis−NIR spectra whose appearance can be correlated with reversible redox couples registered in the corresponding cyclic voltammograms at approximately the same potentials as well as with pronounced evolutions of their resonance Raman spectra. Detailed analysis of the Raman data gives information about the locations and the distribution of radical cations and spinless dication in the macromolecule. This approach can provide a new insight into the formation of high-spin states in these polymers.

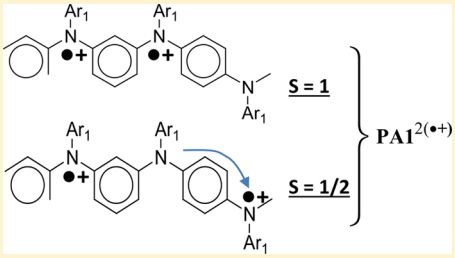

INTRODUCTION

The search for purely organic magnetic materials, especially polymeric ones, which can be applied in molecular electronics or spintronics has attracted considerable attention in the past decade. The main design principles of high-spin polymeric compounds can be outlined as follows: their macromolecules should contain chemical units bearing unpaired spins, separated by conjugated units which can couple these spins in a ferromagnetic fashion.[1] A large variety of spin bearing units has been developed and studied to date, as, for example, triarylmethyl,[2−7] phenoxyl,[8] nitronyl nitroxide,[9,10] aminyl radicals[11−13] and triarylamine radical cations.[14−22] The most impressive result, concerning the fabrication of purely organic ferromagnetic materials, was obtained by Rajca et al. for a polymer containing triarylmethyl radicals which exhibited very high-spin states up to $S = 5000$ at low temperatures.[5] However, considering potential applications of organic magnetic materials, the research should be directed toward the design and synthesis of compounds in which spin bearing units are more stable at room temperature, as, for example, triarylamine radical cations. Recently, several types of alternating oligo- and polyarylamines exhibiting a high-spin state have been synthesized.[14−22] The highest spin state $S = 9/2$ was achieved for cross-linked polyarylamine.[23] Many fundamental studies have also been devoted to linear polymers whose topology facilitates the determination of the principal factors influencing spin interactions. Linear polymers are also interesting due to their solubility and solution processability. The principal problem in this type of compounds is a limited spin concentration causing a decrease in the extent of their magnetic interactions. Moreover, the results obtained to date show that only spins from two neighboring repeat units participate in the formation of the high-spin state and the magnetic interaction is not spread along the polymer chain.[24,25] The main reason for this finding is related to an unfavorable local conformation which can change the nature of an interaction from ferromagnetic to antiferromagnetic. Additionally, the location of the radical cation within the conjugated amine segment can limit the magnetic interaction. Radical cation can be localized only in a specific part of the conjugated unit significantly decreasing spin density in the ferromagnetic coupler which, in turn, results in decreasing ferromagnetic interactions.

In this context, the elucidation of the nature and location of the formed radical cations, possibly by hyphenated electrochemical−spectroscopic (UV−vis−NIR, Raman) techniques, is of crucial importance. In this paper, we describe the results of such detailed studies carried out for four linear polymers containing aromatic amine segments (*p*-phenylenediamine, bis(*p*-aminophenyl)amine, and diaminocarbazole) altered with either *m*-phenylene or 3,5-pyridine ferromagnetic couplers. Detailed theoretical and experimental analysis of the Raman spectra, obtained for these polymers at their different oxidation states, enabled us to gain a deeper insight into the spin and

Received: November 5, 2014
Revised: December 23, 2014
Published: December 23, 2014

DOI: 10.1021/jp511087j
J. Phys. Chem. B 2015, 119, 1756−1767

charge storage configurations, which is crucial for any prediction of their capability of high-spin-state formation.

EXPERIMENTAL SECTION

Materials. *3,6-Bis(4′-methoxyphenyl)amino-9-hexyl-carbazole.* 1.22 g (3 mmol) of 3,6-dibromo-9-hexyl-carbazole, 0.738 g (6 mmol) of *p*-anizidine, 274.7 mg (0.3 mmol) of $Pd_2(dba)_3$, 560.4 mg (0.6 mmol) of BINAP, and 0.864 g (9 mmol) of sodium *tert*-butoxide were dissolved in 20 mL of dry dioxane under an argon atmosphere. The mixture was stirred and heated at 100 °C for 20 h. Removal of the solvent followed by chromatography on silica gel (ethyl acetate/hexanes, 1:2, then 2:1) resulted in a pale-yellow powder. 1.1 g (2.23 mmol, 74.4% yield). ^{1}H NMR (400 MHz, C_6D_6) δ, 7.65 (d, J = 2.0 Hz, 2H), 7.20 (dd, J = 8.6, 2.0 Hz, 2H), 7.11 (d, J = 8.6 Hz, 2H), 6.94 (d, J = 8.8 Hz, 4H), 6.82 (d, J = 8.8 Hz, 4H), 5.01 (s, 2H), 3.83 (t, J = 7.1 Hz, 2H), 3.38 (s, 6H), 1.58 (q, 2H), 1.22−0.99 (m, 6H), 0.81 (t, J = 6.9 Hz, 3H). ^{13}C NMR (100 MHz, C_6D_6) δ, 154.5, 139.8, 137.5, 136.9, 123.9, 120.0, 119.0, 115.1, 111.6, 109.5, 55.2, 43.2, 31.8, 29.3, 27.2, 22.8, 14.1. IR (cm^{-1}): 3350, 3045, 2952, 2927, 2858, 2830, 1509, 1475, 1439, 1309, 1278, 1256, 1230, 1031, 812. Anal. Calcd for $C_{32}H_{35}N_3O_2$: C, 77.86; H, 7.15; N, 8.51; O, 6.48. Found: C, 77.51; H, 7.03; N, 8.53. m/z 493.

Polymerization Procedure. All polymers studied were prepared using Hartwig−Buchwald catalytic amination of aryl halides. Polycondensation was carried out using the method described by Goodson et al.[26] 0.05 mmol of palladium(II) acetate and 0.15 mmol of tri-*tert*-butylphosphine were mixed with 3 mL of dry toluene and stirred for 15 min. Then, 2.5 mmol of 1,3-dibromoderivative, 2.5 mmol of diaminoderivative, 7.5 mmol of sodium *tert*-butoxide, and 12 mL of toluene were placed in a reaction flask containing the catalyst under an argon atmosphere. The mixture was stirred and heated at 90 °C for 4 days. The crude mixture was cooled to room temperature, and the product was precipitated with 300 mL of methanol. The solid was isolated via filtration and then washed with water and methanol. Low-molecular-weight products were removed by extraction with acetone and then with hexane. The remaining polymeric fraction was then dissolved in a small amount of toluene, precipitated in methanol, filtered, and finally dried in a vacuum.

Characterization. *PA1 and PA2.* All spectroscopic and analytical data concerning these polymers can be found in ref 27.

PA4. 2.5 mmol of 3,5-dibromopyridine and 2.5 mmol of bis[(4′-butylpheny)-4-aminophenyl]-4″-*tert*-butylphenylamine were used for the polycondensation reaction. ^{1}H NMR (400 MHz, C_6D_6) δ, 8.40 (d, J = 2.4 Hz, 2H), 7.30 (t, J = 2.4 Hz, 1H), 7.21−7.19 (m, 4H), 7.08 (d, J = 8.8 Hz, 4H), 6.98 (s, 8H), 6.91 (d, J = 8.4 Hz, 4H), 2.41 (t, J = 7.8 Hz, 4H), 1.49−1.41 (m, 4H), 1.27−1.21 (m, 13H), 0.85 (t, J = 7.4 Hz, 6H). ^{13}C NMR (100 MHz, C_6D_6) δ, 145.7, 145.5, 144.8, 144.0, 141.7, 138.2, 137.2, 129.6, 126.5, 126.0, 125.0, 124.7, 124.2, 120.7, 35.3, 34.2, 33.9, 31.4, 22.6, 14.0. Anal. Calcd for $C_{47}H_{50}N_4$: C, 84.14; H, 7.51; N, 8.35. Found: C, 83.42; H, 7.38; N, 8.17. M_n = 8.9 kDa, M_w = 104.0 kDa.

PK1. 2.5 mmol of dibromobenzene, 2.5 mmol of 3,6-bis(4′-methoxyphenyl)amino-9-hexyl-carbazole, and 0.075 mmol of $Pd_2(dba)_3$ and 0.225 mmol of *t*-Bu_3P were used for the polycondensation procedure. ^{1}H NMR (400 MHz, C_6D_6) δ, 7.91 (s, 2H), 7.39 (d, J = 8.8 Hz, 2H), 7.23−7.17 (m, 5H), 7.08−7.00 (m, 2H), 6.97 (d, J = 8.8 Hz, 2H), 6.76 (d, J = 7.9 Hz, 2H), 6.61 (d, J = 8.8 Hz, 4H), 3.67 (s, 2H), 3.18 (s, 6H), 1.48−1.40 (m, 2H), 1.12−1.04 (m, 6H), 0.81 (t, J = 6.9 Hz, 3H). ^{13}C NMR (100 MHz, C_6D_6) δ, 155.8, 150.6, 142.0, 140.3, 138.3, 126.3, 125.8, 124.1, 119.0, 114.9, 113.3, 109.7, 54.8, 31.7, 29.0, 27.0, 22.8, 14.2. Anal. Calcd for $C_{38}H_{37}N_3O_2$: C, 80.42; H, 6.53; N, 7.41; O, 5.64. Found: C, 79.98; H, 6.52; N, 7.33. M_n = 6.9 kDa, M_w = 56.6 kDa.

Spectroscopic Electrochemical and Spectroelectrochemical Techniques. XPS measurements were carried out at room temperature with an Axis Nova spectrometer from Kratos Analytical with an Al Kα line (1486.6 eV) as the excitation source. Thin layers of polymers were deposited on a glass substrate from chloroform solutions by drop-casting, then dried under a gentle nitrogen flux, and then directly introduced overnight in the sample exchange chamber of the spectrometer.

Survey spectra were acquired at a pass energy of 80 eV and with an energy step of 1 eV. The core level spectra (C 1s, O 1s, and N 1s) were acquired using a constant pass energy mode of 10 eV, to obtain data in a reasonable experimental time (energy resolution of 0.28 eV). The pressure in the analysis chamber was maintained below 10^{-7} Pa. Data analysis was performed using CasaXPS software. The background spectra were considered as Shirley type, and curve fitting was carried out with a mixture of Gaussian−Lorentzian functions. Concerning the calibration, the binding energy for the C 1s hydrocarbons peak was set at 284.8 eV. No surface cleaning, using Ar sputtering, for example, was made. It is known from experience that carbonaceous atmospheric contamination usually occurs on the surface of a given material studied, but in the studied cases, ion sputtering can be suspected of changing the chemical composition of the surface and inducing structural damage.

Raman spectra of neutral and oxidized polymers were recorded on a Renishaw InVia reflex spectrometer (λ_{exc} = 633.0 nm, laser power = 10 mW, 2 μm diameter spot, typical exposure times 60 s) or on a FT Raman Bruker RFS 100 spectrometer with the near-IR excitation line (1064 nm, laser power = 50 mW). All experiments were carried out on films of polymers freshly deposited on a platinum plate by drop-casting. The registered Raman signals frequently showed a pronounced baseline slope as a result of fluorescence, extending from 100 to 1700 cm^{-1}. The baseline seriously drifted upon changes in the electrode polarization potential; in addition, it was affected by the energy of the excitation line. These two factors increased the difficulty in identifying characteristic peaks. Therefore, for the fluorescence correction, a "spline" linear interpolation method was rigorously executed to simulate the shape of the baseline, which significantly improved the quality of all spectra. Fourier transform infrared spectra (FTIR) were recorded on a Bruker Vertex 70 spectrometer (4 cm^{-1}), using the KBr pellet method.

Cyclic voltammograms were registered for thin polymer films drop-cast onto a platinum electrode. The experiments were carried out in a one-compartment electrochemical cell, in a solution of 0.1 M Bu_4NBF_4 in CH_2Cl_2 with Ag/0.1 M $AgNO_3$ in acetonitrile as a reference electrode and a Pt counter electrode. The surface of the Pt disk electrode was 25 mm^2. Raman spectroelectrochemical experiments were carried out in the oxidative mode. The potential of the working electrode was being increased in small increments. After each potential raise, a wait time was applied until the *quasi*-equilibrium state was reached and then the Raman spectrum was registered "in situ". It was assumed that the equilibrium state was reached when the potential change induced current became negligible.

DOI: 10.1021/jp511087j
J. Phys. Chem. B 2015, 119, 1756−1767

Computational Methods. Quantum chemical studies, and more precisely density functional theory calculations, were limited to PA1, PA4, and PK1 as representative examples of the two types of polymers studied. The first step within the computational approach was a conformational search of the elemental subunits of polymers with the molecular mechanics (Amber force field). An approach based on modification of selected torsion angles was used, as implemented in the HyperChem75 program. This first scrutiny enabled the most stable conformers of each sequence of polymers to be determined. Then, these optimized structures were used as input geometries for density functional theory (DFT) calculations, performed with the B3LYP functional, using the 6-31+G(d,p) basis set. Geometry optimizations and harmonic frequency calculations were carried out with the Gaussian 09 package.[28] It should be stressed that the calculations here presented were performed in vacuo. However, from the reasonable agreement between the experimental and calculated frequencies, more expensive quantum chemical calculations were estimated unnecessary.

RESULTS

The chemical structures of the studied polymers are depicted in Chart 1. In order to confirm their molecular structure but also

Chart 1. Chemical Structures of the Investigated Polymers Containing Triarylamine Moieties

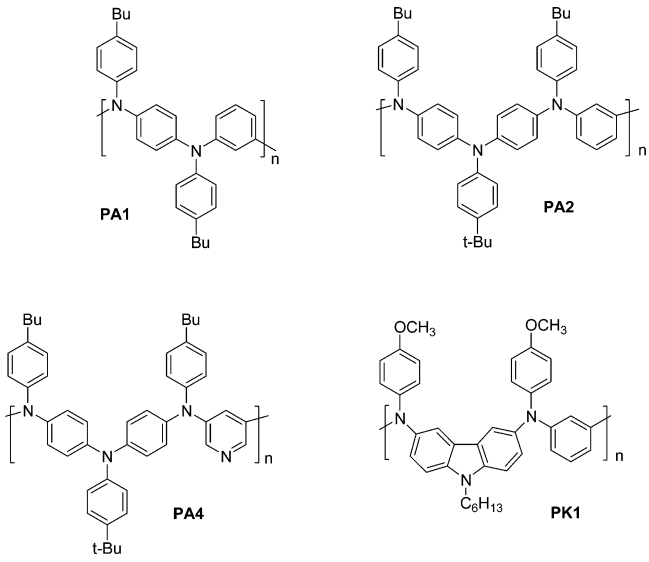

to check that no degradation or partial oxidation took place during the polymerization process, FTIR, Raman spectroscopy, and XPS experiments on as prepared compounds were first conducted.

High-resolution spectra of the XPS core level peaks of C(1s), N(1s), and O(1s) for PA1, PA4, and PK1 are presented in Figure 1 (see Figure S1 in the Supporting Information for the survey data). The C 1s peak is composed of three components at 284.6, 285.0, and 285.6 eV (components 1, 2, and 3, fwhm = 1.1 eV). On the basis of the database, established by Beamson and Briggs,[29] these peaks can be easily assigned to the sp^2 C(H) aromatic carbons, to the saturated hydrocarbons, and to the sp^2 aromatic carbons linked to the nitrogen atoms, respectively. The fourth component at 286.3 eV (numbered 4 in Figure 1) is only observed in the spectrum of PK1, and can be logically

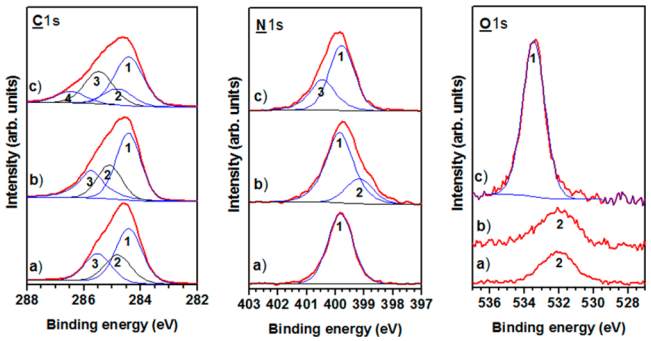

Figure 1. XPS (C 1s, N 1s, and O 1s) spectra of pristine polymers: (a) PA1, (b) PA4, and (c) PK1.

assigned to carbons of the methoxy group. In the N(1s) region, the peak assigned to nitrogen atoms of the triarylamine unit is located at 399.8 eV (fwhm = 1.05 eV). As expected, two additional components are observed in the spectra of PA4 and PK1, i.e., at 399.2 eV (numbered 2) and 400.5 eV (numbered 3), respectively. Unambiguously, they can be assigned to the nitrogen atoms in the pyridine ring and in the alkylcarbazole group. In the O(1s) spectra of PA1 and PA4, they can be attributed to surface contamination, since these molecules do not contain oxygen. The methoxy group in PK1 gives rise to a pronounced, narrow peak at 533.4 eV (fwhm = 1.5 eV). Another point of interest, the $\pi-\pi^*$ shakeup satellite peaks around 291.5 eV, a characteristic of aromatic or conjugated systems, constitute about 2.4−2.7% for PA1, PA4, and PK1, and significantly increase (4.0%) in the spectrum of PA2, which may indicate a higher conjugation in this polymer (see Figure S2, Supporting Information). Finally, Table 1 lists the surface

Table 1. XPS-Determined and Theoretically Calculated Contents in at% (±0.5%) of C, N, O, and Br in Thin Films of PA1, PA2, PA4, and PK1

	C (%)		N (%)		O (%)		
	expt	theo	expt	theo	expt	theo	Br (%)
PA1	94.4	94.1	5.6	5.9	<1.0	0	<0.1
PA2	94.3	94.1	5.7	5.9	<0.6	0	<0.1
PA4	92.6	92.2	7.4	7.8	<1.0	0	<0.1
PK1	88.4	88.4	6	6.9	5.6	4.6	<0.1

elemental analysis (in at%) for all polymers studied, which is compared with theoretically calculated values. No peaks attributable to bromine can be detected, indicating efficient removal of the oligomers. No peaks are found in the spectral range characteristic of N^+(1s) (ca. 402 eV), proving the neutral state of the as prepared polymers. A good agreement between the determined and theoretically calculated contents of all elements in these polymers should be pointed out.

Another point of interest was to elucidate the molecular structure of pristine polymers by combining the results of quantum chemical calculations and compare with the data obtained by vibrational spectroscopies. It is well-known that all features of Raman scattering and infrared absorption spectra are signatures of the molecular structure, since they are determined by the conformation of the molecule (macromolecule) and the distribution of the valence electron density. Therefore, all changes in the fingerprints of a given molecule (macromolecule) can be considered as an indication of the evolution in its electronic and/or conformational structure. However, in

DOI: 10.1021/jp511087j
J. Phys. Chem. B 2015, 119, 1756−1767

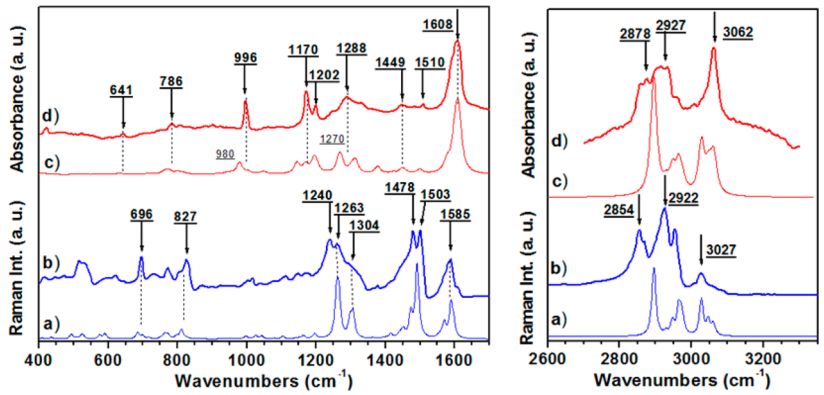

Figure 2. Raman scattering and infrared absorption spectra of pristine PA1: (a) computed infrared absorption spectrum; (b) experimental infrared absorption spectrum (powder in KBr pellet); (c) simulated Raman spectrum; (d) experimental Raman spectrum (thin film, λ_{exc} = 1064 nm).

Table 2. Raman Frequencies (in cm^{-1}) of the Main Vibrational Modes of PA1, PA2, and PA4 in Their Neutral State[a]

Raman scattering experimental and computed bands (cm^{-1})				benzene	pani[31]	
PA1		PA2	PA4	Wilson notation	ν (cm^{-1})	
expt	calc	expt	expt	calc	expt	assignments
3062	3066			3068 (2, 13)		aromatic C−H stretch
3045	3050			3063 (20)		
3027	3030			3047 (7)		
2955	2968					CH_2, CH_3 stretch (aliphatic groups)
2922	2950					
2854	2896					
1608	1604	1608	1605	1596 (8a)	1618	C−C stretch + C−H bend para and meta disubstituted benzene ring
			1578			
1587	1596	sh.	sh.	1596 (8b)	1597	C−C stretch + C−H bend (intraring)
1570	1570					
1510	1490	1507	1507	1486 (19a)	1497	ring stretch + deformation
1449	1452	1449				methyl and methylene H−C−H def.
1328		1334		1326 (3)	1340	ring stretch
1288	1267	1288	1288		1219	C−N stretch + C−C stretch (interring) and *tert*-butyl deformation (1250 cm^{-1})
1245		1250	sh.			
1202	1190	1202	1202	1178 (9a)	1181	aromatic C−H bend (para and meta parasubstituted benzene ring)
1170	1164	1170	1170			
	1150		1152			
996	980	994	1015	1010 (12)		ring deformation (meta disubstituted ring)
786	810	786	786	849 (10)	867	C−H deformation (out of plane)
	772	752	752			aromatic C−H wag (o.p.)

[a]Vibrational modes of polyaniline, reported in ref 31, are given for comparison.

this approach, the main experienced difficulty is often to find the attribution of the Raman and IR peaks, and then to interpret these complex spectroscopic data in terms of molecular structure. Therefore, the support of quantum chemistry calculations is frequently needed.

In Figure 2, Raman scattering and infrared absorption spectra (IR) of PA1 are shown as representative examples. The spectra of other polymers are similar, with small differences arising from the presence of the pyridine linker in PA4 and the carbazole group in PK1. The calculated spectra consisting of Lorentzian-shape peaks (Figure 2a and c) are compared with the experimental ones (Figure 2b and d). It should be noted that computed frequency values contain known systematic errors, resulting in overestimates. Therefore, it is usual to scale the theoretically predicted frequencies by an empirical factor of 0.965. In addition, the width of the Lorentzian lines has to be adjusted to approximate the appearance of the actual spectra (the fwhm was set to 6 cm^{-1} for Raman and 10 cm^{-1} for infrared absorption spectra). Despite the fact that the DFT calculations were performed in the gas-phase environment, which should be considered as a very approximate assumption, the agreement with the experimental data turned out to be good enough for straightforward interpretation and understanding the spectroscopic data.

The attributions of vibrational modes of the studied polymers, listed in Table 2 (Raman scattering peaks) and Table S1 in the Supporting Information (IR absorption peaks), were done with the support of previous publications,[30−33] appropriate reference books,[34,35] and exploiting the DFT modeling. The results presented in this table are largely self-explanatory, so the discussion is limited to the bands which showed pronounced evolutions during the spectroelectrochem-

DOI: 10.1021/jp511087j
J. Phys. Chem. B 2015, 119, 1756−1767

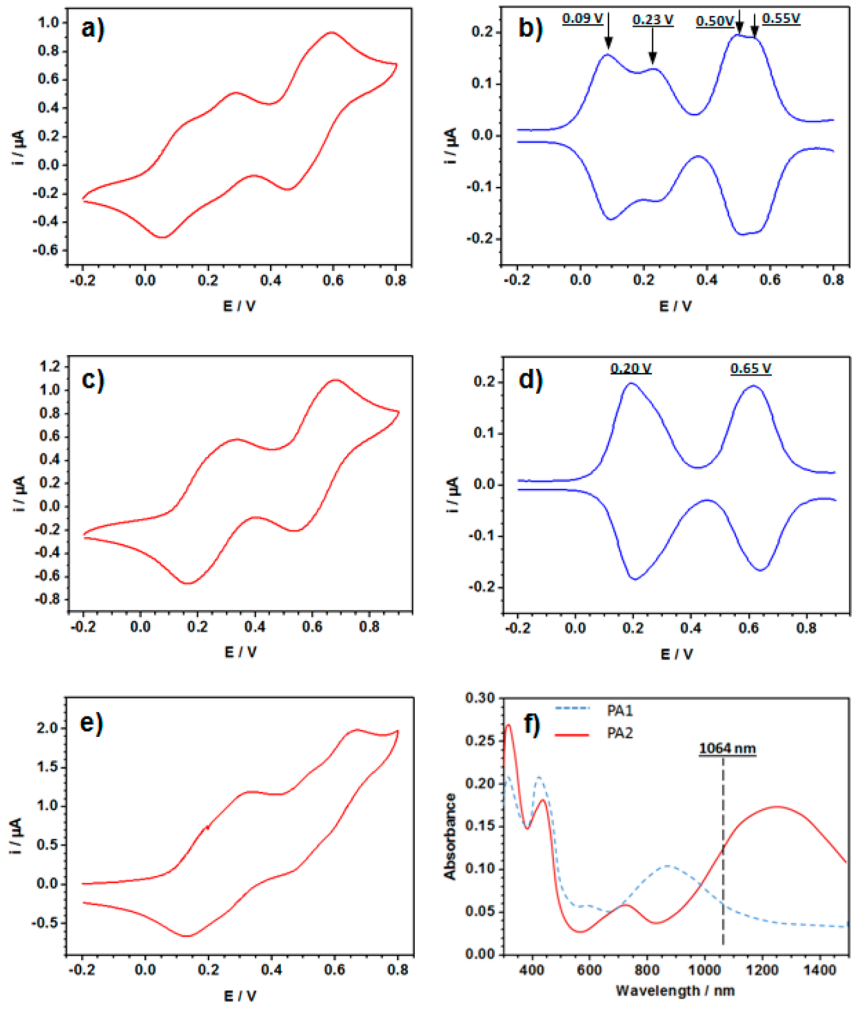

Figure 3. Cyclic voltammograms obtained for (a) PA2, (c) PA4, and (e) PK1 in 0.1 M Bu_4NBF_4/dichloromethane (scan rate 50 mV/s, *E* vs Ag/$AgNO_3$ 0.1 M in acetonitrile). (b and c) Differential pulse voltammograms obtained for PA2 and PA4, respectively. (f) Optical absorption spectra of PA1 and PA2 after their electrochemical oxidation.

ical experiments (*vide infra*). The Raman scattering and infrared absorption data of all four polymers are presented in the Supporting Information (Figures S3 and S4). In the case of PK1, no exploitable Raman spectra could be registered, neither at λ_{exc} = 633 nm nor at 1064 nm, because of strong fluorescence.

The most characteristic features of the calculated and registered Raman spectra can be outlined as follows: (i) two strongly overlapping, sharp peaks at 1595 and 1610 cm^{-1} can unambiguously be assigned to the aromatic C−C stretching deformations, consistent with the neutral state of the polymers; (ii) a clear band at 1288 cm^{-1} is usually attributed to the C−N stretching in aromatic amines,[33,36] which is also confirmed by the DFT calculations; (iii) a weak band at ca. 1202 cm^{-1} together with a band at ca. 1170 cm^{-1} is characteristic of the C−H in-plane bending deformations in the aromatic ring; (iv) a band pointed at 996 cm^{-1} which is always absent in a para-substituted benzene ring confirms the coexistence of meta-substituted rings. It should be stressed the shift of this mode to 1015 cm^{-1} in the spectrum of PA4 is due to the presence of a pyridine ring. Some additional bands can be observed at 1449 cm^{-1}, i.e., in the spectral range characteristic of CH_2/CH_3 deformations of the aliphatic groups and in the 2500−3500 cm^{-1} range, assigned to different aliphatic (sp^3) C−H or aromatic (sp^2) C−H stretching bands, as assigned in Table 2. All the assignments were confirmed by the examination of the vibration modes (Cartesian displacements) of the main modes, modeled by quantum chemical calculations.

In a similar manner, careful inspection of the infrared absorption spectra of all four polymers studied reveals the presence of peaks characteristic of aromatic rings (para- and meta-substituted) and of amine groups at 1263 and 1240 cm^{-1}. As already mentioned, the assignments of the experimental spectra were confronted with theoretical predictions and vibration descriptions. For instance, in Figure 2, where the experimental and computed vibrational spectra of PA1 are presented on the same graph, despite the inherent assumptions of our calculations, the agreement between the experimental and modeling data is acceptable, at least for the aim established in this research. In addition, the complementarity of these two spectroscopies can easily be noticed. The observed exclusion of some modes is surprising if the lack of symmetry of the repeat units of the studied polymers is considered. However, it can be assumed that the local environment of the meta- or para-substituted benzene ring retains a pseudosymmetry of C_{2v} or D_{2h} point groups, respectively. Finally, all other assignments can be found in Table 2, with the associated number in Wilson notation.

DOI: 10.1021/jp511087j
J. Phys. Chem. B 2015, 119, 1756−1767

In addition to the vibrational study, the macromolecule geometries have been optimized. The following features of this optimization should be noted: The phenyl rings are assumed to be flat and identical, with ∠CCC angles and ∠CCH angles of exactly 120°. The values for the bond lengths are reported in agreement with the averaged values obtained from spectroscopic and X-ray crystallographic studies of TPA (triphenylamine) in the solid state.[37,38] The C−N distance and the ∠CNC angle are computed as 1.422 Å and 120°, and the angle by which the phenyl groups are rotated relative to the plane defined by the C−N bonds is found between 35 and 45°.

All studied polymers can be oxidized to radical cations. Cyclic voltammetry is a useful research tool for studying the oxidation processes in electrochemically active polymers and for understanding their redox properties. In Figure 3a, c, and e, cyclic voltammograms of thin layers of PA2, PA4, and PK1, drop-cast on a platinum plate from a dichloromethane solution, are presented, whereas the cyclic voltammogram of PA1 can be found in ref 27.

The cyclic voltammograms show two to three strongly overlapping oxidation peaks in the potential range from −0.2 to 0.8 V vs $Ag/AgNO_3$ (see Figure 3 and Table 3 for the measured redox potential values). The differential pulse measurements (Figure 3b and d and Figure S5 in the Supporting Information) reveal the presence of reversible redox couples.

Table 3. Redox Potentials of the Studied Polymers

polymer	E_{ox1} (V)[a]	E_{ox2} (V)	E_{ox3} (V)	E_{ox4} (V)
PA1	0.18	0.33	0.76	0.86
PA2	0.09	0.23	0.50	0.55
PA4	0.20	0.62		
PK1	0.18	0.28	0.50	0.61

[a]The values of the oxidation potentials are given vs Ag/Ag^+.

In the cases of the voltammograms registered for PA1, PA2, and PK1, the first two oxidation peaks can be attributed to the removal of two electrons from two neighboring conjugated moieties separated by an *m*-phenylene ring (see Table 4). In the voltammogram of PA4, the first oxidation peak is very broad and can also be attributed to the oxidation of two adjacent conjugated segments; however, the values of the oxidation potentials are very close; thus, their separation cannot be detected even using the differential pulse technique. The third and fourth peaks observed in the voltammograms of PA1, PA2, and PK1 correspond to the removal of a second electron from each of the two neighboring conjugated moieties. A similar process can be attributed to the second oxidation peak in the PA4 voltammogram. Thus, the last processes can lead to the formation of two positive charges in each conjugated segment, which can be preserved in the form of two radical cations or a spinless imine dication. Using vibrational spectroscopy, we tried to elucidate this problem.

Table 4. UV−vis−NIR Spectroscopic Data for the Studied Polymers in Their Neutral and Oxidized States

polymer	neutral state (nm)	oxidized state (nm)
PA1	318	427, 610, 870
PA2	323	440, 725, 1250
PA4	321	421, 750, 1180
PK1	310	485, 822, 2340

As already reported, the formation of radical cations can be investigated using UV−vis−NIR spectroscopy. The identification of the oxidation-induced absorption bands is very important because in Raman spectroscopy the positions as well as the intensities of the bands may be strongly affected by the change of the resonance conditions during the spectroelectrochemical experiment. Therefore, in the interpretation of the Raman resonant spectra, evolution of the optical absorption bands in the course of the polymer oxidation must be taken into account. In Figure 3f, the UV−vis−NIR spectra registered for PA1 and PA2, oxidized at a constant potential of E = 0.4 V vs $Ag/AgNO_3$, are presented. In these experiments, the potential of 0.4 V was applied to the working electrode until the quasi-equilibrium state was reached. Then, the electrode was removed from the electrochemical cell and the optical measurements were performed *ex situ*. It should be noted that absorption spectra of pristine PA1 and PA2 show only one band at ca. 320 nm, which is attributed to the $\pi-\pi^*$ transition in the phenylene ring.[27] Oxidation of these polymers yields new bands attributable to radical cations and dications (see Table 4).

Due to luminescence problems when using the visible excitation lines, we have focused on Raman spectroelectrochemistry performed with λ_{exc} = 1064 nm. This choice is also fully justified by the Raman resonance or preresonance conditions of the electrochemically oxidized macromolecules.

Figure 4a presents Raman spectra of PA1 as a function of the electrochemical working electrode potential. The intensity of the Raman scattering quickly increases with increasing E, in

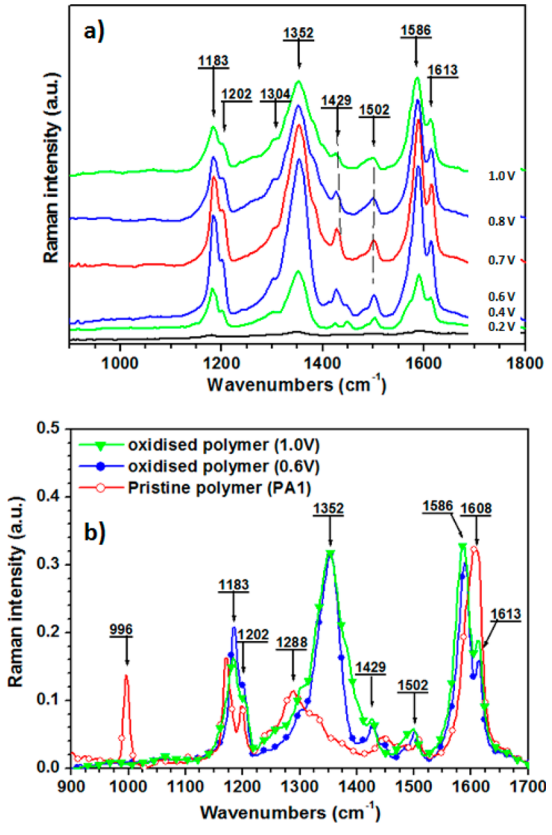

Figure 4. (a) Raman spectra of PA1 registered for increasing working electrode potentials, E vs $Ag/AgNO_3$ 0.1 M in acetonitrile. (b) Comparison of Raman spectra of PA1 in the pristine, partially and fully electrochemically oxidized forms (λ_{exc} = 1064 nm).

DOI: 10.1021/jp511087j
J. Phys. Chem. B 2015, 119, 1756−1767

agreement with the evolution of the optical absorption. Simultaneously, a decrease of the fluorescence allows easier extracting of the Raman signal from the background.

Although all registered spectra look similar, their careful inspection reveals some significant differences. To follow the evolution of the characteristic bands upon the electrochemical oxidation, in Figure 4b, the vibrational fingerprints of the oxidized molecule are compared to those of pristine PA1. First, an evolution of the band at 1608 cm^{-1} is observed which is now split into two new peaks pointed at 1586 and 1613 cm^{-1}. Second, the band at 1288 cm^{-1} disappears in favor of a strong and wide band pointed at 1352 cm^{-1}. The characteristic aromatic band at 1165 cm^{-1} is shifted to 1183 cm^{-1}, and the characteristic band of the meta-substituted ring is no longer observable at 996 cm^{-1}. For higher potential (E = 1.0 V), two new peaks in a form of shoulders appear at 1164 and 1386 cm^{-1} (Figure 4b). They will be discussed in a subsequent part of the paper.

The structure of PA2 differs from that of PA1 by the number of structurally nonequivalent nitrogens because PA2 has two different types of nitrogen (Scheme 1). In PA1, all nitrogens are

Scheme 1. Chemical Structures of PA2 and the Numbering of Nitrogen Atoms

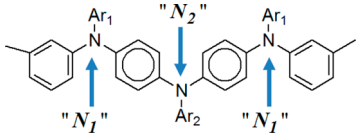

connected to one meta-substituted phenylene ring and two para-substituted ones. In PA2, one out of three nitrogens in the repeat unit are connected to three para-substituted aromatic rings. Moreover, PA2 shows better conjugation than PA1, as evidenced by the position of the optical absorption bands and by lower values of its oxidation potentials.

Several issues arise: Are we able to identify and to differentiate between the radical cations generated on the two different nitrogen sites using Raman spectroscopy? Are we able to determine whether the first polarons are localized on N1 or N2 sites (see Scheme 1)? Are we able to predict the various localized deformations of the structural units in the vicinity of the introduced charges?

Figure 5 shows Raman spectra of PA2 registered for increasing working electrode potentials. Their close inspection reveals three consecutive evolutions of the spectra. First, for potential $E \leq 0.4$ V, the spectra are characterized by broad overlapping bands in the spectral range from 1550 to 1620 cm^{-1} with two maxima pointed at 1605 and 1613 cm^{-1}. The positions of these two peaks are very close to those registered for the neutral form of PA2. In addition, a new broad band appears at 1352 cm^{-1}, together with a band of smaller intensity at ca. 1280 cm^{-1}. Moreover, an intensive band consisting of two or three components grows with a maximum at 1176 cm^{-1}. In the second step of the oxidation, for the potentials $E_{ox} \geq 0.4$ V, the spectra show a significant evolution with the emergence of an intensive peak at 1586 cm^{-1}. The peak at 1496 cm^{-1} grows in intensity, and an intensive band at ca. 1350 cm^{-1} broadens and shifts toward higher energies (1380 cm^{-1}). At this step, the spectra become very similar to those registered for PA1, despite the persistence of some differences.

From these observations, it can be affirmed that the emergence of radical cations in PA2 does not exactly follow the same evolutions as in the case of PA1. This suggests that the nitrogen atoms "N2" (Scheme 1), which are absent in PA1, play an important role in the oxidation processes, especially at low electrode polarization potentials. For $E \geq 0.5$ V, the Raman spectra of PA2 closely resemble those registered for PA1. It can therefore be postulated the charges are mainly localized on "N1" nitrogens. Finally, for high working electrode potentials, widening of the bands attributed to CN valence bonds could indicate the presence of dications (spinless bipolaron). In addition, it should be emphasized here that, at a fixed potential, the simultaneous presence of several components in the bands indicates the coexistence of different structures. We will develop this point in the Discussion section (*vide infra*).

To analyze the radical cation localization within the conjugated unit, we have also studied PA4, which contains a pyridine linker and PK1 in which an alkyl carbazole group is integrated into the repeat unit. Considering the chemical properties of pyridine, one can suppose that its presence in the polymer chain should repulse positive charges of radical cations, leading to their localization in the center of the conjugated unit. Contrary, a planar structure of carbazole should increase the delocalization of radical cation generated in PK1. Thus, in both polymers, opposite effects of radical cation localization should be observed. Thus, new questions arise: Where will the charges introduced into the polymer chain during the electrochemical oxidation be located? Which nitrogen atoms will mainly bear

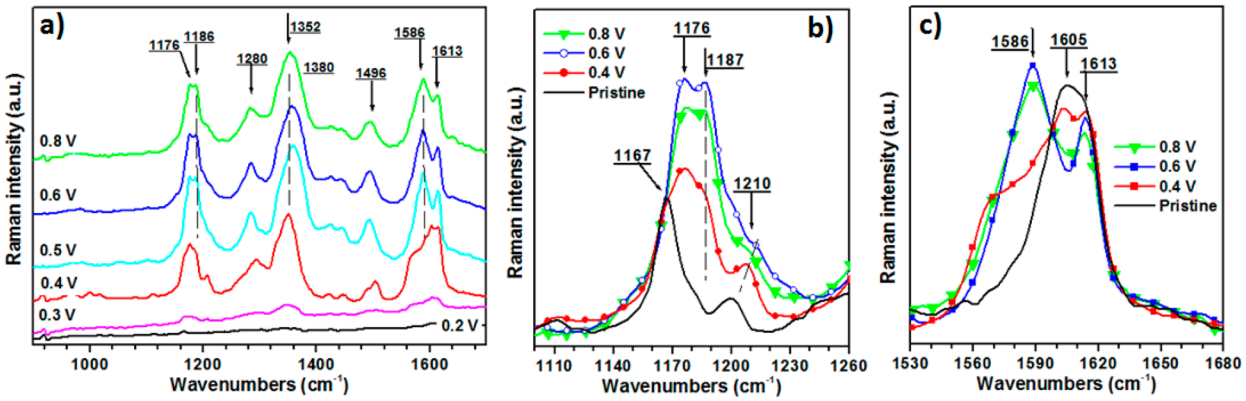

Figure 5. Raman spectra of PA2 registered for increasing working electrode potentials, E vs $Ag/AgNO_3$ 0.1 M in acetonitrile, λ_{exc} =1064 nm: (a) wide spectra; (b and c) enlarged zone of aromatic CH vibrations (bending) and aromatic C−C vibrations (stretching).

DOI: 10.1021/jp511087j
J. Phys. Chem. B 2015, 119, 1756−1767

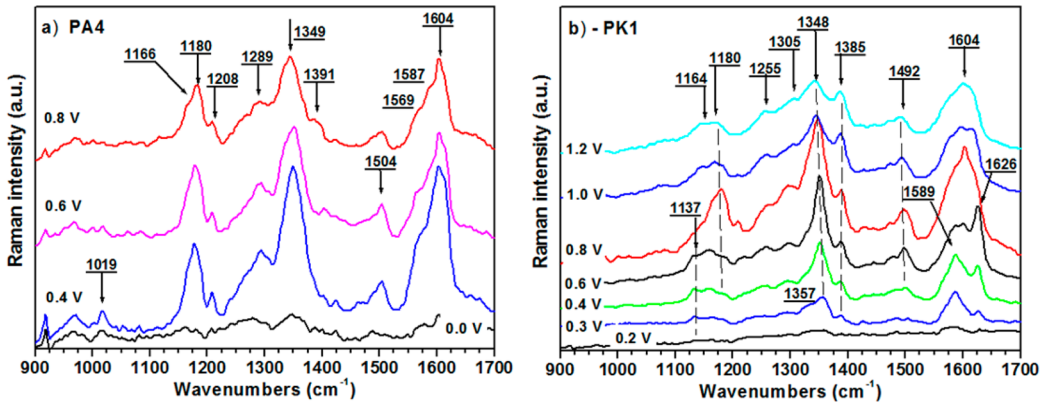

Figure 6. Raman spectra of (a) PA4 and (b) PK1 as a function of the oxidation potential (λ_{exc} = 1064 nm).

radical cations? What is the new organization of the modified polaron/bipolaron lattice?

Careful analysis of Raman spectra recorded during the electrochemical oxidation of PA4 and PK1 can bring the answer. It is clear from Figure 6 that the evolutions of the spectra are very different in both cases. For instance, for PA4, only one type of spectrum is observed, and it corresponds to that registered for PA2 at low working electrode potentials (E < 0.4 V). Indeed, the main bands are pointed at 1180, 1289, 1349, and 1604 cm^{-1}. It can therefore be assumed that radical cations are exclusively located on "N2" nitrogen atoms. Probably, the presence of pyridine rings results in pushing off the radical cations to prevent the formation of positive charges in their vicinity.

On the contrary, Raman spectra of PK1 shown in Figure 6b are more complex, containing rich information that uniquely defines the multiple aspects of the polymer electronic structure. A careful analysis of these spectra shows three main steps in the electrochemical oxidation of PK1. Below 0.4 V, the recorded spectra are very close to that of PA1. The $CN^{\bullet+}$ band at 1357 cm^{-1} is sharp, and the main band appears at 1589 cm^{-1}. Logically, it can be assumed that the first radical cations are located on N1 amine nitrogen atoms, close to the meta-substituted aromatic ring. The interpretation of the spectra recorded at potentials between 0.6 and 0.8 V is more difficult. Actually, the spectrum recorded at E = 0.6 V can be characterized by a relative increase of the band at 1626 cm^{-1}, while the spectrum registered at E = 0.8 V is marked by the domination of bands at 1180 and 1604 cm^{-1}. For higher working electrode potentials, the emergence of the band at 1380 cm^{-1} can be noticed together with the presence of several components in the bands located around 1180 and 1600 cm^{-1}. Finally, it should be stressed here that, unlike the pyridine ring, alkyl-carbazole contributes positively to the formation of radical cations, and it can even be assumed that the nitrogen atom in the carbazole unit also supports the formation of charge carriers; thus, the planar structure of carbazole facilitates the radical cation delocalization. All of these observations confirm the coexistence of different structures, as will be explained in the Discussion section (*vide infra*).

DISCUSSION

The aim of this study is to understand the formation of radical cations in four different polyarylamines. In general, *m*-phenylene (or *m*-pyridine) rings can be considered as ferromagnetic couplers of spins created in the conjugated units. It has been determined that in the case of PA1 mainly uncoupled (S = 1/2) spins are present with some fraction of S = 1 spins. For PA2, almost the pure triplet state S = 1 was observed.[25] In PA4, only uncoupled spins (S = 1/2) were detected, and for PK1, a mixture of S = 1 (mainly) and S = 1/2 was registered (unpublished data). We suppose that the formation of high-spin state depends on the local conformation of the polymer chain as well as on the localization/delocalization of the radical cation within the conjugated units. Thus, we believe that Raman spectroscopy can bring important information about the location of the spins and charges in these systems. It can therefore provide a better understanding of the complex mechanisms involved in the formation of high-spin states.

On the basis of careful analysis of the Raman spectra of PA1, the following mechanism can be postulated: when the first radical cation $PA1^{\bullet+}$ is created (see Scheme 2), the local environment of the nitrogen atom is perturbed and the CN stretch vibration is shifted to 1350 cm^{-1}. In addition, as shown in Figure 7, the following spectral changes can be noticed: the emergence of a narrow band at 1184 cm^{-1} (the aromatic CH bending, mode *9a*) together with two bands at 1333 and 1355 cm^{-1} (C–N stretching mode region) and a strong peak at 1585 cm^{-1} accompanied by a smaller one at 1613 cm^{-1}.

Scheme 2. Chemical Structures of PA1 Oxidized to Radical Cations

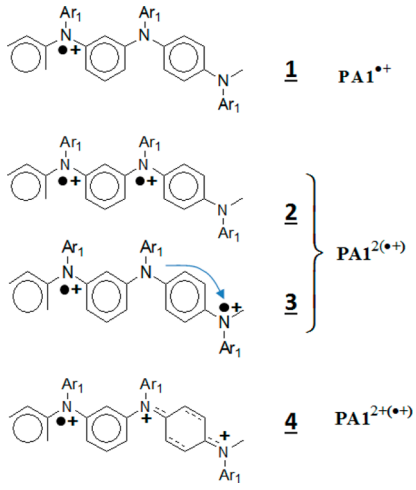

DOI: 10.1021/jp511087j
J. Phys. Chem. B 2015, 119, 1756–1767

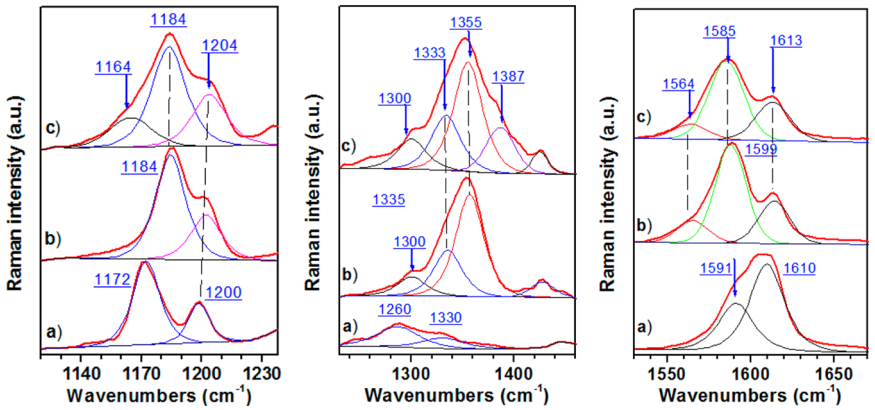

Figure 7. Raman spectra of PA1: (a) pristine; (b) oxidized at E = 0.4 V vs Ag/Ag^+; (c) oxidized at 0.8 V vs Ag/Ag^+.

During the creation of the second radical cation, two structures can be suggested ($PA1^{2(\bullet+)}$). The first one, numbered 2 in Scheme 2, presents an S = 1 spin state. However, due to the charge repulsion, and the presence of a conjugated segment, the polaron can be moved on the neighboring nitrogen atom, thereby drastically decreasing the coupling between spin sites. In this way, the spin state decreases to S = 1/2 (majority of spin states). All of these structures present the same Raman features, because in these three configurations only one positive charge is created per one conjugated segment. These characteristic bands are reported in Table 5. To the contrary, when a second electron is withdrawn from a short conjugated segment, i.e., at higher working electrode potentials, two new bands appear at 1164 and 1387 cm^{-1}, probably derived from the association of two radical cations to form a spinless dication (S = 0). As already shown in the literature,[39] this association promotes an important electron−lattice coupling and causes a strong local geometric distortion in the molecules, as represented by structure 4 in Scheme 2.

Table 5. Raman Frequencies (in cm^{-1}) of the Main Vibrational Modes of PA1, PA2, PA4, and PK1 in Their Oxidized State

	PA1	PA2	PA4	PK1
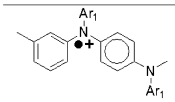	1613	1613	1615	1627
	1585	1586	1589	1587
	1564	1571	1563	1570
	1355	1355	1355	1355
	1333	1336	---	1328
	1184	1187	1187	1182
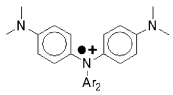		1599	1502	
		1567	1563	
		1355	1355	
		1336	1336	
		1174	1176	
			1164	
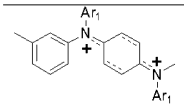	1387	1372		1387
	1164	1155		1144
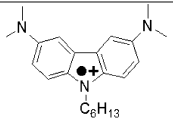				1602
				1350
				1325

In the case of PA2, the observed changes are more complex. Decomposition of Raman bands, presented in Figure 8, clearly indicates the coexistence of three structures, even for low working electrode potentials. These decompositions were conducted using the Gaussian−Lorentzian mix function (ratio 30:70) and after subtraction of the background. The peak positions of all samples were reproducible using a fixed fwhm (or under attentive control). However, it should be stressed that, unlike in the case of XPS, and because the selective resonance effects are difficult to evaluate, the relative amount of each species cannot be assessed by integration of the peak area. Two steps of the oxidation process, at different electrode potentials, can be derived from the Raman data (Figure 8). In the first step, the radical cation $PA2^{\bullet+}$ created in a conjugated segment is highly delocalized, which is manifested by the position and the shape of the NIR band in the UV−vis−NIR spectrum. However, the high intensities of the Raman bands at 1599 and 1174 cm^{-1} observed for the polymer oxidized at $E \leq$ 0.5 V suggest that the radical cation is more localized on the N2 nitrogen atom than on N1 (Scheme 1), which is also supported by the spin density distribution calculated by Hirao et al.[40] for conjugated triamine. To support this assumption, we can note that these new Raman bands do not coincide exactly with those observed for PA1.

In addition to these new bands, Raman spectra present bands observed in the spectrum of PA1 (1187, 1355, and 1586 cm^{-1}) (Figure 8). From these observations, it is possible to propose the following mechanism: When the first electron is removed from the conjugated segment, the radical cation is mainly located on the central nitrogen ("N2"), as represented in Scheme 3, structure 1 ($PA2^{\bullet+}$); however, the presence of a radical cation on "N1" nitrogens is also possible, which leads to magnetic interactions of coextensive spin densities via a meta-phenylene ring to form the S = 1 state.[25] When a second electron is then pulled out, two structures can be proposed: the formation of two radical cations $PA2^{2(\bullet+)}$ located on "N1" nitrogens, separated by charge repulsion (structure 2, Scheme 3), or the creation of a spinless dication $PA2^{2+}$ (structure 3, Scheme 3). It should be stressed here that structure 3 is thermodynamically more stable than structure 2; for this reason, our previous pulsed-EPR measurements showed a

DOI: 10.1021/jp511087j
J. Phys. Chem. B 2015, 119, 1756−1767

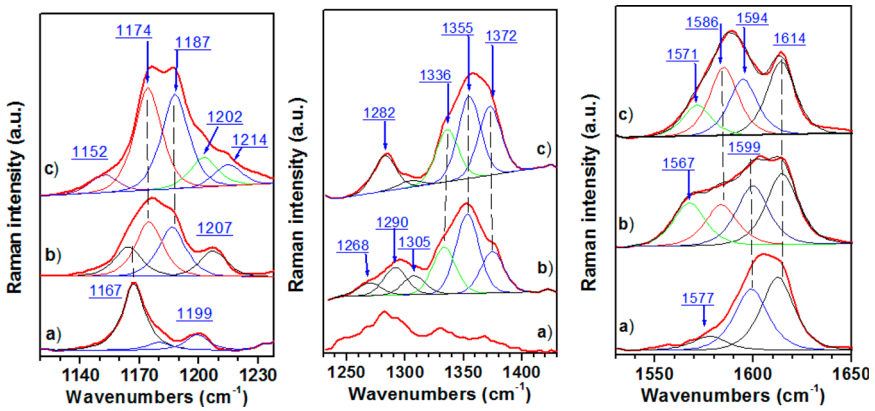

Figure 8. Raman spectra of PA2: (a) pristine; (b) oxidized at 0.4 V; (c) oxidized at 0.8 V.

Scheme 3. Chemical Structures of PA2 Oxidized to Radical Cations

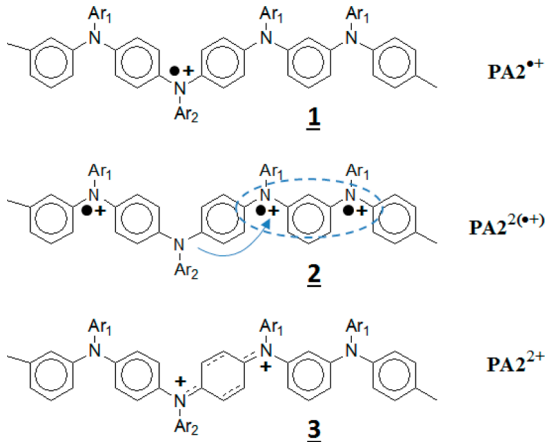

significant decrease of triplet spin states for the highly oxidized polymer.[25]

Contrary to the above case, the repulsion of positive charges caused by the presence of pyridine rings in PA4 leads to a decrease of spin density on "N1" nitrogen atoms, pushing the radical cation toward the "N2" site. This assumption is fully consistent with the prevailing presence of Raman bands at 1176 and 1602 cm^{-1} (see Figure S6, Supporting Information). In addition, the bands at 1159 and 1575 cm^{-1} attest to the presence of a pyridine ring, with unchanged frequencies even for high potentials of the working electrode. Thus, only uncoupled spins ($S = 1/2$) are detected for this polymer. However, some important local conformation of the polymer chain, especially caused by the rotation of the amine group linked to the pyridine ring, which should also influence the magnetic properties, cannot be excluded in this case.

PK1 represents the most complex case. Raman spectra of this polymer oxidized below 0.4 V show an increase of the relative intensities of the band located at 1182, 1355, and 1618 cm^{-1} (Figure S7 in the Supporting Information), thus supporting the conclusion that the radical cation is mostly located on amine nitrogens. However, the planar structure and the electron-donating effect of the carbazole group can induce the delocalization of the radical cation in the entire conjugated unit. One can observe the bands at 1602 cm^{-1} and the displacement of the 1355 cm^{-1} band to 1347 cm^{-1}. This could be indicative of the radical cation location on carbazole nitrogen. In addition, as already seen in the spectra of PA2, the Raman bands registered for oxidized PK1 are very broad, comprised of several contributions. This observation confirms the coexistence of different kinds of charges, probably located on different parts of the polymer chain (see Figure S8 in the Supporting Information). If the characteristic bands of the radical cations and dications located on different nitrogens atoms (N1 and N2) are correctly identified, some new Raman bands tend to prove that the radical cations and dications are also localized on the carbazole moiety (see Table 5).

CONCLUSION

To summarize, in this work, we have studied four different alternating polymers of aromatic amines and meta-phenylene (or pyridine). Complementary spectroscopic, electrochemical, and spectroelectrochemical investigations have shown that the oxidation process is associated with the formation of radical cations or dications located in different parts of the macromolecule. Careful analysis of the Raman spectra indicated that the formed radical cation is located on the N1 nitrogen atom in the oxidized polymer PA1 whereas on the N2 site in oxidized PA4 which contains a pyridine moiety. In the case of PA2 and PK1, radical cations created in oligoamine segments are more delocalized in the entire conjugated unit. However, one radical cation created in the conjugated segment is more localized on N2 than on the N1 site in PA2, whereas in PK1 they are more localized on N1 than on the carbazole nitrogen. We suppose that spectroscopic studies could lead to crucial conclusions concerning the interaction of spins generated in these polymers. The accurate Raman band analysis gives a better understanding of the complex mechanisms involved in the formation of high-spin state due to the fact that the formation of this state depends on the local conformation of the polymer chain as well as on the relative localization of the radical cation within conjugated units.

ASSOCIATED CONTENT

Supporting Information

XPS (survey) spectra of pristine PA1, PA2, PA4, and PK1; XPS (C 1s) spectra of PA2; Raman scattering and infrared absorption data of pristine polymers; Raman spectra of oxidized PA4 and PK1; chemical structures of PK1 oxidized to radical cations; and table of infrared absorption frequencies. This material is available free of charge via the Internet at http://pubs.acs.org.

DOI: 10.1021/jp511087j
J. Phys. Chem. B 2015, 119, 1756−1767

AUTHOR INFORMATION

Corresponding Authors

*E-mail: guy.louarn@cnrs-imn.fr. Phone: 33-240 376 327.
*E-mail: ikulsz@ch.pw.edu.pl. Phone: 48-22-2345584.

Notes

The authors declare no competing financial interest.

ACKNOWLEDGMENTS

I.K.-B. and L.S. wish to acknowledge financial support from National Centre of Science in Poland (NCN, Grant No. UMO-2011/01/B/ST5/03903) and the Foundation for the Polish Science (TEAM/2011-8/6). G.L. and H.d.S. express their acknowledgment to the Spectroscopy Resource Center (SPEC) at the PROPPG/UEL, the Special Visiting Researcher Program (PVE) run by CAPES (Project no. 124/2012), and the Brazilian Research Centre (CNPq) and CAPES for their financial support.

REFERENCES

(1) Bujak, P.; Kulszewicz-Bajer, I.; Zagorska, M.; Maurel, V.; Wielgus, I.; Pron, A. Polymers for Electronics and Spintronics. *Chem. Soc. Rev.* **2013**, *42*, 8895−8999.

(2) Rajca, A.; Rajca, S.; Wongsriratanakul, J. Very High-Spin Organic Polymer: π-Conjugated Hydrocarbon Network with Average Spin of S ≥ 40. *J. Am. Chem. Soc.* **1999**, *121*, 6308−6309.

(3) Rajca, A.; Wongsriratanakul, J.; Rajca, S. Organic Spin Clusters: Macrocyclic-Macrocyclic Polyarylmethyl Polyradicals with very High Spin *S* = 5−13. *J. Am. Chem. Soc.* **2004**, *126*, 6608−6626.

(4) Rajca, S.; Rajca, A.; Wongsriratanakul, J.; Butler, P.; Choi, S. M. Organic Spin Clusters. A Cendritic-Macrocyclic Poly (arylmethyl) Polyradical with very High Spin of *S* = 10 and its Derivatives: Synthesis, Magnetic Studies, and Small-Angle Neutron Scattering. *J. Am. Chem. Soc.* **2004**, *126*, 6972−6986.

(5) Rajca, A.; Wongsriratanakul, J.; Rajca, S. Magnetic Ordering in an Organic Polymer. *Science* **2001**, *294*, 1503−1505.

(6) Rajca, A. From High-Spin Organic Molecules to Organic Polymers with Magnetic Ordering. *Chem.—Eur. J.* **2002**, *8*, 4834−4841.

(7) Rajca, A. Organic Diradicals and Polyradicals: From Spin Coupling to Magnetism? *Chem. Rev.* **1994**, *94*, 871−893.

(8) Kaneko, T.; Makino, T.; Miyaji, H.; Teraguchi, M.; Aoki, T.; Miyasaka, M.; Nishide, H. Ladderlike Ferromagnetic Spin Coupling Network on a π-Conjugated Pendant Polyradical. *J. Am. Chem. Soc.* **2003**, *125*, 3554−3557.

(9) Oka, H.; Tamura, T.; Miura, Y.; Teki, Y. Synthesis and Characterization of Poly(1,3-phenylene)-based Polyradicals Carrying Cyclic Aminoxyls. *J. Mater. Chem.* **2001**, *11*, 1364−1369.

(10) Oka, H.; Tamura, T.; Miura, Y.; Teki, Y. Synthesis and Characterization of Poly(1,3-phenylene)-Based Polyradical Carrying Cyclic Nitroxides. Observation of Ferromagnetic Interaction. *Polym. J.* **1999**, *31*, 979−982.

(11) Rajca, A.; Olankitwanit, A.; Rajca, S. Triplet Ground State Derivative of Aza-m-xylylene Diradical with Large Singlet - Triplet Energy Gap. *J. Am. Chem. Soc.* **2011**, *133*, 4750−4753.

(12) Rajca, A.; Boratyński, P. J.; Olankitwanit, A.; Shiraishi, K.; Pink, M.; Rajca, S. Ladder Oligo (m-aniline) s: Derivatives of Azaacenes with Cross-Conjugated π-Systems. *J. Org. Chem.* **2012**, *77*, 2107−2120.

(13) Rajca, A.; Olankitwanit, A.; Wang, Y.; Boratyński, P. J.; Pink, M.; Rajca, S. High-Spin *S* = 2 Ground State Aminyl Tetraradicals. *J. Am. Chem. Soc.* **2013**, *135*, 18205−18215.

(14) Ito, A.; Ino, H.; Tanaka, K.; Kanemoto, K.; Kato, T. Facile Synthesis, Crystal Structures, and High-Spin Cationic States of All-para-Brominated Oligo(N-phenyl-m-aniline)s. *J. Org. Chem.* **2002**, *67*, 491−498.

(15) Maurel, V.; Jouni, M.; Baran, P.; Onofrio, N.; Gambarelli, S.; Mouesca, J. M.; Djurado, D.; Dubois, L.; Desfonds, G.; Kulszewicz-Bajer, I. Magnetic Properties of a Doped Linear Polyarylamine Bearing a High Concentration of Coupled Spins (S = 1). *Phys. Chem. Chem. Phys.* **2012**, *14*, 1399−1407.

(16) Bushby, R. J.; Taylor, N.; Williams, R. A. Ferromagnetic Spin-Coupling 4,4″-through Metaterphenyl: Models for High-Spin Polymers. *J. Mater. Chem.* **2007**, *17*, 955−964.

(17) Bushby, R. J.; Kilner, C. A.; Taylor, N.; Vale, M. E. Disjoint and Coextensive Amminium Radical Cations: a General Problem in Making Amminium Radical Cation Based High-Spin Polymers. *Tetrahedron* **2007**, *63*, 11458−11466.

(18) Bushby, R. J.; McGill, D. R.; Ng, K. M.; Taylor, N. Disjoint and Coextensive Diradical Diions. *J. Chem. Soc., Perkin Trans.* **1997**, *2*, 1405−1414.

(19) Wienk, M. M.; Janssen, R. A. J. Stable Triplet-State Di(Cation Radicals) of a Meta−Para Aniline Oligomer by "Acid Doping". *J. Am. Chem. Soc.* **1996**, *118*, 10626−10628.

(20) Wienk, M. M.; Janssen, R. A. J. High-Spin Cation Radicals of Meta−Para Aniline Oligomers. *J. Am. Chem. Soc.* **1997**, *119*, 4492−4501.

(21) van Meurs, P. J.; Janssen, R. A. J. Ferromagnetic Spin Alignment in Head-to-Tail Coupled Oligo(1,4-phenyleneethynylene)s and Oligo-(1,4-phenylenevinylene)s Bearing Pendant p-Phenylenediamine Radical Cations. *J. Org. Chem.* **2000**, *65*, 5712−5719.

(22) Michinobu, T.; Takahashi, M.; Tsuchida, E.; Nishide, H. Robust Triplet Molecule: Cationic Diradical of 3,4′-Bis(diphenylamino)-stilbene. *Chem. Mater.* **1999**, *11*, 1969−1971.

(23) Michinobu, T.; Inui, J.; Nishide, H. m-Phenylene-linked Aromatic Poly(aminium cationic radical) s: Persistent High-spin Organic Polyradicals. *Org. Lett.* **2003**, *5*, 2165−2168.

(24) Maurel, V.; Jouni, M.; Baran, P.; Onofrio, N.; Gambarelli, S.; Mouesca, J. M.; Djurado, D.; Dubois, L.; Jacquot, J. F.; Desfonds, G.; Kulszewicz-Bajer, I. Magnetic Properties of a Doped Linear Polyarylamine Bearing a High Concentration of Coupled Spins (*S* = 1). *Phys. Chem. Chem. Phys.* **2012**, *14*, 1399−1407.

(25) Dobrzynska, E.; Jouni, M.; Gawrys, P.; Gambarelli, S.; Mouesca, J. M.; Djurado, D.; Dubois, L.; Wielgus, I.; Maurel, V.; Kulszewicz-Bajer, I. Tuning of Ferromagnetic Spin Interactions in Polymeric Aromatic Amines via Modification of Their π-Conjugated System. *J. Phys. Chem. B* **2012**, *116*, 14968−14978.

(26) Goodson, F. E.; Hauck, S. I.; Hartwig, J. F. Palladium-catalyzed Synthesis of Pure, Regiodefined Polymeric Triarylamines. *J. Am. Chem. Soc.* **1999**, *121*, 7527−7539.

(27) Gałecka, M.; Wielgus, I.; Zagorska, M.; Pawłowski, M.; Kulszewicz-Bajer, I. High-Spin Radical Cations of Poly(m-p-anilines) and Poly(m-p-p-anilines): Synthesis and Spectroscopic Properties. *Macromolecules* **2007**, *40*, 4924−4932.

(28) Frisch, M. J.; et al. *Gaussian 09*, revision A.02; Gaussian, Inc.: Wallingford, CT, 2009.

(29) Beamson, G.; Briggs, D. *The Scienta ESCA 300 Database. High Resolution XPS of Organic Polymers*; John Wiley & Sons: New York, 1992.

(30) Wilson, E. B., Jr. The Normal Modes and Frequencies of Vibration of the Regular Plane Hexagon Model of the Benzene Molecule. *Phys. Rev.* **1934**, *45*, 706−714.

(31) Quillard, S.; Louarn, G.; Lefrant, S.; MacDiarmid, A. G. Vibrational Analysis of Polyaniline: a Comparative Study of Leucoemeraldine, Emeraldine, and Pernigraniline Bases. *Phys. Rev. B* **1994**, *50*, 12496−12508.

(32) Boyer, M. I.; Quillard, S.; Cochet, M.; Louarn, G.; Lefrant, S. RRS Characterization of Selected Oligomers of Polyaniline in situ Spectroelectrochemical Study. *Electrochim. Acta* **1999**, *44*, 1981−1987.

(33) Kulszewicz-Bajer, I.; Louarn, G.; Djurado, D.; Skorka, L.; Szymanski, M.; Mevellec, J.-Y.; Rols, S.; Pron, A. Vibrational Dynamics in Dendridic Oligoarylamines by Raman Spectroscopy and Incoherent Inelastic Neutron Scattering. *J. Phys. Chem. B* **2014**, *118*, 5278−5288.

(34) Dollish, F. R.; Fateley, W. G.; Bentley, F. F. *Characteristic Raman Frequencies of Organic Compounds*; John Wiley & Sons: New York, 1974.

DOI: 10.1021/jp511087j
J. Phys. Chem. B 2015, 119, 1756−1767

(35) Varsányi, G. *Vibrational Spectra of Benzene Derivatives*; Academic Press: New York, 1969; pp 17−84.
(36) Rai, G.; Kumar, A. K.; Rai, S. Infrared, Raman Spectra and DFT Calculations of Chlorine Substituted Anilines. *Vib. Spectrosc.* **2006**, *42*, 397−402.
(37) Meijer, G.; Berden, G.; Meerts, W. L.; Hunziker, H. E.; de Vries, M. S.; Wendt, H. R. Spectroscopy on Triphenylamine and its Van Der Waals Complexes. *Chem. Phys.* **1992**, *163*, 209−222.
(38) Sobolev, A. N.; Belsky, V. K.; Romm, I. P.; Chernikova, N. Y.; Guryanova, E. N. Structural Investigation of the Triaryl Derivatives of the Group V Elements. IX. Structure of Triphenylamine, C18H15N. *Acta Crystallogr., Sect. C* **1985**, *41*, 967−971.
(39) Salaneck, W. R.; Friend, R. H.; Brédas, J. L. Electronic Structure of Conjugated Polymers: Consequences of Electron−Lattice Coupling. *Phys. Rep.* **1999**, *319*, 231−251.
(40) Hirao, Y.; Ito, A.; Tanaka, K. Intramolecular Charge Transfer in a Star-Shaped Oligoarylamine. *J. Phys. Chem. A* **2007**, *111*, 2951−2956.

DOI: 10.1021/jp511087j
J. Phys. Chem. B 2015, 119, 1756−1767